



Effect of torsional ground motion on seismic response of symmetric multistorey buildings incorporating soil–structure interaction

JAVED AHMAD BHAT^{1,*}, G V RAMANA² and A K NAGPAL²

¹National Institute of Technology Srinagar, Srinagar, Kashmir 190006, India

²Department of Civil Engineering, Indian Institute of Technology Delhi, Hauz Khas, New Delhi 110016, India

e-mail: bhat_javed@nitsri.ac.in; ramana@civil.iitd.ernet.in; aknagpal@civil.iitd.ernet.in

MS received 12 January 2022; revised 29 June 2022; accepted 30 June 2022

Abstract. Effect of torsional ground motion is considered in the seismic codes indirectly by considering accidental eccentricity which also includes uncertainties in storey masses and stiffnesses of structural elements of the buildings. However, there is no explicit mention of the effect of torsional ground motion on the response for different types of buildings including soil–structure interaction (SSI), as it is reported in the literature that torsionally flexible low-rise buildings are susceptible to torsional ground motion. A systematic study has been carried out on the effect of torsional ground motion including SSI on the response of torsionally flexible through torsionally stiff multistorey buildings. The effect of torsional ground motion resulting from the propagation of motion through different soil mediums: firm soil, medium-firm soil and soft soil is reported in the study. For these soil mediums, two cases of ground motion: (i) translation ground motion only and (ii) combined translation and torsional ground motion are considered. A set of multistorey buildings with fundamental period of vibration $T = 0.3$ s and $T = 0.8$ s having frequency ratios $\Omega = 0.65, 1.0$ and 1.5 ($\Omega =$ ratio of uncoupled fundamental torsional frequency, ω_θ to uncoupled fundamental translational frequency, ω_t) is considered. These chosen buildings cover practically the entire spectrum of torsionally flexible and torsionally stiff low-rise buildings. Frequency domain analysis has been carried out to incorporate SSI effects. The results obtained from the frequency domain have been transformed into the time domain using Fast Fourier Transform (FFT) and the storey shears obtained from ten earthquake time histories (translation and torsional) have been averaged. It is found that the torsional ground motion effect is significant in the case of torsionally flexible buildings with low periods of vibration and the effect of SSI is insignificant in all types of buildings. Further, the combined effect of torsional ground motion and soil–structure interaction on the distribution of storey shears along the height varies significantly for high period buildings ($T = 0.8$ s).

Keywords. Torsional ground motion; multistorey buildings; seismic response; spatial variation; earthquake time history; soil–structure interaction.

1. Introduction

Recorded translational ground motion histories are available but no actual records of the rotational ground motion have been obtained till date. Kozák [1] reported that seismic torsional motion effects might be responsible for the distortion of an obelisk in the San Bruno monastery following the 1783 Calabria earthquake and many illustrations and observations as evidence of the effect of rotational ground motions were presented. Zerva *et al* [2] reported that torsional ground motion may be the potential contributing factor that may affect the seismic response of structural systems. Even though the studies regarding the torsional ground motions date back to the mid-nineteenth

century, the torsional component of ground motion has been considered only in a limited number of studies. The effect of spatial variation of ground motion (torsional ground motion) on the response of structures has also been considered by taking translational ground motions at individual supports. Spatial variation of the ground motion that produces torsion was considered by applying it to individual supports of symmetric, mono asymmetric and two-way asymmetric buildings [3–6].

The effect of torsional ground motion on the response of structures was studied and it was found that there is a significant increase in the response for buildings with low fundamental periods T and low frequency ratios Ω ($\Omega =$ ratio of uncoupled fundamental torsional frequency, ω_θ to uncoupled fundamental translational frequency, ω_t) [7, 8]. Similarly, Hao [9] reported that effect of torsional ground

*For correspondence

motion is significant for lower values of T and lower values of apparent wave velocity, V_a , (function of shear wave velocity, V_s and angle of incidence of propagating waves, θ). Very limited work on the effect of torsional ground motion including soil-structure interaction (SSI) effects is reported. Spatial variation of ground motion (wave passage effect only) has been considered by taking different time lags in translational ground motions at the supports of a plane frame, incorporating SSI, [10]. However, the torsional response reported in these studies is based on a model of single storey building.

For multistorey buildings subjected to torsional ground motion, some studies have been reported, [11–13]. These studies have been carried out on highly torsionally stiff symmetric multistorey frame buildings for different aspect ratios (length to width ratio of the building). As expected only a small effect had been found on such types of buildings. Similarly, Basu *et al* and Loghman *et al* [14, 15] investigated the seismic behaviour of seismically isolated buildings subjected to rotational components of ground motions. It is reported that the response of seismically isolated buildings could be significantly amplified due to torsional ground motion [14], whereas, Loghman *et al* [15] reported 33.75% amplification in the base shear and 120% amplification in roof acceleration due to the inclusion of torsional ground motion in the buildings that have a square plan and higher slenderness ratio. They also observed that the effect of torsional ground motion on roof acceleration increases for the buildings that have higher aspect ratios. In another study, Basu *et al* [16] proposed an alternative procedure that accounts for both accidental eccentricity produced due to uncertainties in mass and stiffness distribution as well as torsional ground motions. Recently, Guidotti *et al* [17] have reported an increase of 15% in inter-story drift in tall buildings due to the inclusion of near field ground motions with their torsional components. Further, it is reported that the effect of torsional ground motion on the floor acceleration of structures with a relatively short torsional period of vibration may be significant [18]. Compilation of analytical studies and findings associated with the response of structures due to torsional ground motion have been reported by Anagnostopoulos *et al* [19] in a review paper. In these studies it was concluded that overall seismic response of structures with varying dynamic properties and, with various geometric irregularities could be adversely affected by the torsional components of ground motions. In all these studies [12, 13, 19] the effect of torsional ground motion on the seismic response of multistorey buildings has been reported. Recently effect of torsional ground on the response of multistorey buildings with fixed foundation is reported by Bhat *et al* [20, 20]. In this study it is reported that there is a significant increase in the response of flexible buildings with low period of vibration. However, there is no study available that has taken into account the effects of soil

medium i.e. incorporating SSI effects and torsional ground motion.

Practically no work is available in literature on the distribution of storey shears along the height of multistorey buildings subjected to torsional ground motion and incorporating SSI. A comprehensive study for multistorey buildings subjected to torsional ground motion incorporating SSI is required, to take into account the effect of governing parameters: V_s or V_a (soil type), Ω and T on the distribution of storey shears along the height of stiffening elements of these buildings. In this paper, studies are reported in this direction.

Systematic studies have been carried out for the entire range of governing parameters for the low-rise buildings for which the effect of torsional ground motion is significant. The values of structural properties of buildings for chosen values of pairs of parameters T and Ω are arrived at by an iterative process.

2. Simulation of earthquake ground motions

Due to the absence of appropriate sensors, it is neither possible nor feasible to measure torsional ground motion directly and reliably [14, 21, 22]. Therefore, many researchers have derived torsional ground motion from their translational components using kinematic source models or the elasto-dynamic theory of wave propagation. Three analytical methods were proposed by Basu *et al* [14] to extract rotational components of ground motions from their translational components. Torsional accelerograms compatible with artificial translational accelerograms with a given proportion of surface and body waves were also developed, [23]. But none was tested against an estimated torsional ground motion from field measurements. De La Llera and Chopra [7, 8] estimated the torsional ground motion numerically at the basement of 30 buildings during the 1994 earthquakes of California. Similarly, torsional ground motions were also estimated numerically using recorded spatially varying translational ground motions, [21, 24–26]. But no explicit formula for estimating torsional ground motion was presented. Hao [9] estimated torsional ground motion numerically from SMART-1 array and presented a power spectral density function (psdf) of the torsional ground motion at a point on the ground surface taking both phase shift and coherency loss effect into consideration. This torsional psdf was verified with psdf of estimated torsional ground motion obtained from actual records of translation from SMART-1 array. The proposed power spectral density function for torsional acceleration is of the form given below and has been used for the simulation of torsional ground motions in the present study.

$$S_{\theta Z}(\omega) = S_g(\omega)\omega \left\{ \alpha_1(\omega) + \alpha_2(\omega) + \frac{\omega}{2V_a^2} \right\} \quad (1)$$

where $S_g(\omega)$ = translational motion (acceleration) power spectral density function, V_a = apparent wave velocity of the propagating wave and $\alpha_1(\omega)$ & $\alpha_2(\omega)$ frequency dependent parameter functions that take into account the coherency loss effect and are expressed in the form

$$\alpha_j(\omega) = \frac{a_j}{\ln(\omega) + b_j}, \omega \geq 0.314 \frac{rad}{s}, j = 1, 2 \quad (2)$$

in which a_j and b_j are determined by the regressive method from the recorded motions of SMART-1 array. Three sets of values for a_j and b_j for low, medium and high coherency have been proposed in [9]: $a_j = 1.0 \times 10^{-7}$, $b_j = 1.16$, $j = 1, 2$ for high coherency, $a_j = 5.0 \times 10^{-6}$, $b_j = 2.00$, $j = 1, 2$ for low coherency and $a_1 = 1.1160 \times 10^{-6}$, $b_1 = 1.66726$, $a_2 = 1.1593 \times 10^{-6}$, $b_2 = 1.72263$, for medium coherency. The values of a_j and b_j ($j = 1, 2$) corresponding to medium coherency have been used in the present study.

The apparent wave velocity V_a , is a function of shear wave velocity of the medium V_s and angle of incidence θ of the propagating wave with the vertical and is expressed as

$$V_a = \frac{V_s}{\sin(\theta)} \approx \frac{V_s}{0.87\phi} \quad (3)$$

where ϕ (in radians) = principal direction of the ground motion.

The values of ϕ , V_s and corresponding V_a have been reported by O'Rourke *et al* [27] for the San Fernando earthquake in February 1971.

The translational motion power spectral density function used by Hao [9] in the derivation of torsional psdf is a filtered Tajimi-Kanai spectrum and has been used in the present study.

$$S_g(\omega) = \left[\frac{1 + 4\xi_g^2 \left(\frac{\omega}{\omega_g}\right)^2}{\left[1 - \left(\frac{\omega}{\omega_g}\right)^2\right]^2 + 4\xi_g^2 \left(\frac{\omega}{\omega_g}\right)^2} \right] \times \frac{\left(\frac{\omega}{\omega_s}\right)^4}{\left[1 - \left(\frac{\omega}{\omega_s}\right)^2\right]^2 + 4\xi_s^2 \left(\frac{\omega}{\omega_s}\right)^2} S_0 \quad (4)$$

where S_0 = scale factor depending on the ground motion intensity, ω_g and ω_s = central ground frequency and central frequency of high pass filter in rad/s respectively and ξ_g and ξ_s = damping at central ground frequency and damping at central filter frequency respectively.

Hindy and Novak [28] proposed values of ω_s/ω_g and ξ_g/ξ_s as 0.1 and 1.0, respectively. For different soil conditions values of ω_g and ξ_g have been reported, [9, 29]. The values of ω_g for the three types of soils, firm soil, medium-

firm soil and soft soil were respectively presented as: $\omega_g = 31.416$ rad/s, 15.70 rad/s and 6.283 rad/s respectively [9]. The values of ξ_g adopted in the study have been taken as $\xi_g = 0.35, 0.45$ and 0.55 for firm soil, medium-firm soil and soft soil respectively, [29].

The translational motion (acceleration) psdf for firm, medium-firm and soft soils are shown in figure 1(a). The corresponding torsional motion (acceleration) psdf are shown in figure 1(b) for $\theta = 10^\circ$. From the psdf of translational ground motion it is seen that a large amount of energy is present over a broader frequency band for firm soil and medium-firm soil, whereas for soft soil the energy is centered in a narrow band due to the filtering of higher frequencies. From the torsional ground motion psdf it is seen that the energy is distributed over a large frequency range in comparison to the translational motion psdf.

Earthquake ground motions (translation/torsion) have been simulated assuming that any periodic function, $\ddot{u}_g(t)$ can be expanded into a series of sinusoidal waves having random phase angles uniformly distributed between 0 and 2π and having amplitudes determined from the power spectral density function, which can be expressed as

$$\ddot{u}_g(t) = \sum_{j=1}^N A_j \sin(\omega_j t + \Phi_j) \quad (5)$$

where A_j = amplitude, ω_g = frequency in rad/s and Φ_j = phase angle of j th sinusoidal wave distributed between 0 and 2π . The amplitudes of j th sinusoidal wave with frequency interval $\Delta\omega$ are given by: $A_j = \sqrt{4S\Delta\omega}$, where S = power spectral density function of the ground motion (S_g for translational ground motion and $S_{\theta z}$ for torsional ground motion).

The transient character of an earthquake can be accounted for by multiplying the periodic function $\ddot{u}_g(t)$ by an envelope function. The envelope function used, is a Bogdanoff type, and the final expression for the generation of the simulated earthquake time histories (translation/torsion) in the present study is

$$\ddot{u}_g(t) = a t e^{-bt} \sum_{j=1}^N A_j \sin(\omega_j t + \Phi_j) \quad (6)$$

where $a = 0.206$ and $b = 0.0078$ are two constants. Torsional ground motions are out of phase by $-\pi/2$ from translational ground motions, [21, 30]. Thus, a phase difference of $-\pi/2$ is introduced in Eq (6) for torsional ground motion.

Velocity response spectra are developed here to validate the ground motion time histories generated, based on Eq (6), for $\Omega = 1.0$ and peak ground acceleration, $pga = 1g$. These spectra are in good agreement when compared with those reported by Hao [9] (figure 2).

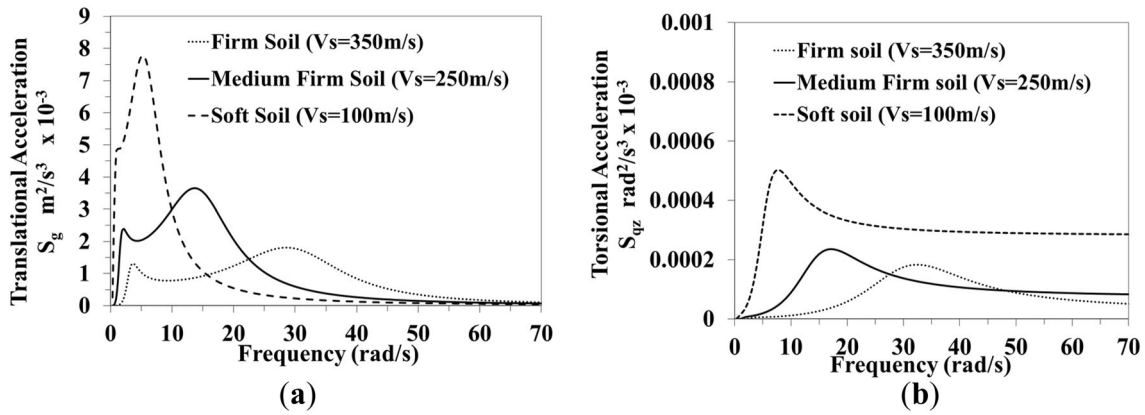


Figure 1. Power spectral density function: (a) translational motion psdf, (b) torsional motion psdf.

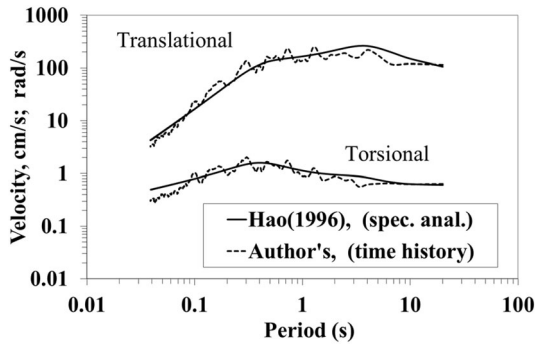


Figure 2. Comparison of velocity response spectra for translation and torsion: ($Va=1000$ m/s; $\omega_g=2.5$ Hz.; $\xi_g=0.6$; $pga=1.0$ g).

3. Modeling and equations of motion

Multistorey buildings comprising of frames as stiffening elements are considered. Floor slabs of these buildings are assumed to have infinite in-plane rigidity and no bending stiffness. Mass of each storey is lumped at the corresponding floor level. Figure 3 shows the superstructure-foundation system (interaction system) consisting of the superstructure and the raft as foundation system. As shown in figure 3b each floor is assumed to have 3 degrees of freedom (d.o.f.); a translation along each of the two orthogonal axes in the plane of the floor and a rotation about a vertical axis through the c.g. (centre of gravity) of the raft. The raft is assumed to have 5 d.o.f. (figure 3c), a translation along each of the two orthogonal axes in the horizontal plane, a rotation about each of the two axes and a rotation about the vertical axis again through the c.g. of the raft. The interaction system is subjected to horizontal free field motion in x or y directions and torsional ground motion about the z -axis.

The superstructure-foundation system is treated as two substructures: superstructure and foundation. The

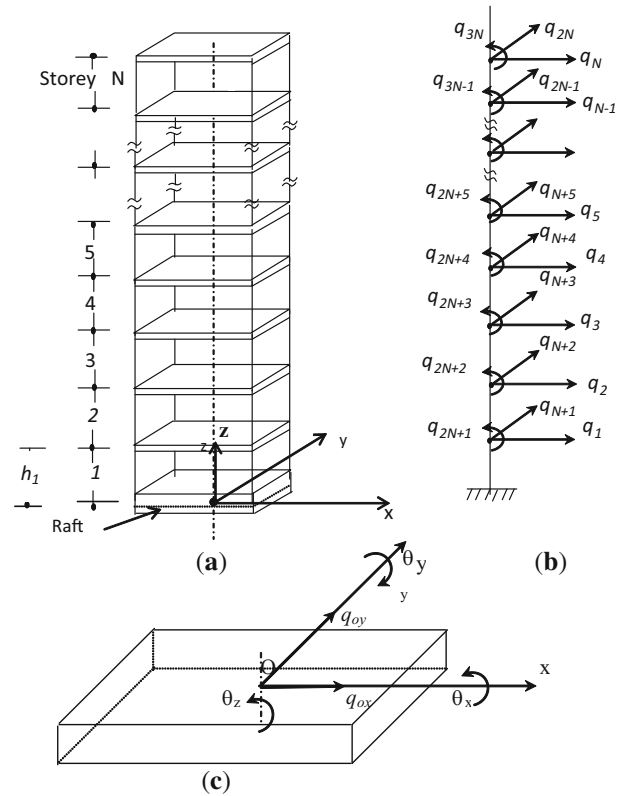


Figure 3. Interaction system of building model: (a) schematic presentation of building, (b) degrees of freedom in global coordinates and (c) degrees of freedom of the raft.

governing equations of motion are written separately for each substructure.

3.1 Equations of motion for the superstructure

Displacements at any floor level result from the movement of the raft and the structural displacements of the floor with

respect to the raft. The contribution to the floor displacements, $\{q^r\}$ from the movement of the raft is given by

$$\{q^r\} = [A]\{q_g\} + [B]\{q_o\} \quad (7)$$

in which, $\{q_g\}^T = \{q_{gx} \ q_{gy} \ q_{\theta_z}\}$, where q_{gx} and q_{gy} are free field translational ground motions in x and y directions respectively and q_{θ_z} is the torsional ground motion about the z -axis, $\{q_o\}^T = \{q_{0x} \ q_{0y} \ \theta_y \ \theta_x \ \theta_z\}$, in which q_{0x} and q_{0y} are translations of the raft in x and y directions respectively and

θ_x , θ_y and θ_z are rotations of the raft about x , y and z axes respectively and matrices A ($3N \times 3$) and B ($3N \times 5$) are of the form

$$[A]^T = \begin{bmatrix} 111\dots 1 : & 000\dots 0 : & 000\dots 0 \\ 000\dots 0 : & 111\dots 1 : & 000\dots 0 \\ 000\dots 0 : & 000\dots 0 : & 111\dots 1 \end{bmatrix}$$

$$[B]^T = \begin{bmatrix} 111\dots 1 : & 000\dots 0 : & 000\dots 0 \\ 000\dots 0 : & 111\dots 1 : & 000\dots 0 \\ 000\dots 0 : & 000\dots 0 : & 111\dots 1 \\ h_1 h_2 h_3 \dots h_N : & 000\dots 0 : & 000\dots 0 \\ 000\dots 0 : & h_1 h_2 h_3 \dots h_N : & 000\dots 0 \\ 000\dots 0 : & 000\dots 0 : & h_1 h_2 h_3 \dots h_N \end{bmatrix}$$

where $h_i = (1 \text{ to } N) =$ height of i th floor from the c.g. of the raft, figure 3.

As stated earlier in addition to the above displacements, floors undergo structural displacements relative to the raft; let $\{q\}$ be the vector of structural displacements. Equations of motion of the superstructure now are

$$[M]\{\ddot{q}\} + [C]\{\dot{q}\} + [K]\{q\} = 0 \quad (8)$$

where $[M]$, $[K]$ and $[C]$ are mass, stiffness and damping matrices in global co-ordinates respectively. The total displacement vector, $\{q^r\}$ can be expressed as

$$\{q^r\} = \{q^r\} + \{q\} \quad (9)$$

Substituting $\{q^r\}$ and $\{q^r\}$ from Eq. 7 and Eq. 9, Eq. 8 becomes

$$[M]\{\ddot{q}\} + [M][B]\{\ddot{q}_0\} + [C]\{\dot{q}\} + [K]\{q\} = -[M][A]\{\ddot{q}_g\} \quad (10)$$

3.2 Equations of motion for the raft

The raft is acted upon by the forces from the superstructure as well as the reactive forces from the soil. The equations of equilibrium of the raft can be expressed as

Translation along x -direction:

$$\sum_{i=1}^N m_i \ddot{q}_i^x + \sum_{i=1}^N (-m_i y_{ci}) \ddot{q}_{2N+i}^x + m_0 (\ddot{q}_{gx} + \ddot{q}_{0x}) + V_{fx} = 0 \quad (11a)$$

Rotation about y -axis:

$$\sum_{i=1}^N m_i \ddot{q}_i^y h_i + \sum_{i=1}^N (-m_i y_{ci}) h_i \ddot{q}_{2N+i}^y + \ddot{\theta}_y \sum_{i=0}^N I_{yi} + M_{fy} = 0 \quad (11b)$$

Translation along y -direction:

$$\sum_{i=1}^N m_i \ddot{q}_{N+i}^y + \sum_{i=1}^N (m_i x_{ci}) \ddot{q}_{2N+i}^y + m_0 (\ddot{q}_{gy} + \ddot{q}_{0y}) + V_{fy} = 0 \quad (11c)$$

Rotation about x -axis:

$$\sum_{i=1}^N m_i \ddot{q}_{N+i}^x h_i + \sum_{i=1}^N (m_i x_{ci}) h_i \ddot{q}_{2N+i}^x + \ddot{\theta}_x \sum_{i=0}^N I_{xi} + M_{fx} = 0 \quad (11d)$$

Rotation about z -axis:

$$\sum_{i=1}^N m_i (-y_{ci} \ddot{q}_i^z + x_{ci} \ddot{q}_{N+i}^z) + \sum_{i=1}^N [m_i (y_{ci}^2 + x_{ci}^2) + I_{zi}] \ddot{q}_{2N+i}^z + (\ddot{q}_{\theta_z} + \ddot{\theta}_z) I_{z0} + M_{fz} = 0 \quad (11e)$$

where \ddot{q}_i^x = total acceleration at the i^{th} floor, m_0 = raft mass, I_{xi} , I_{yi} , and I_{zi} = mass moment of inertia of the raft ($i = 0$) and of floors ($i = 1 \text{ to } N$) about x , y and z axis respectively. x_{ci} and y_{ci} are the coordinates of center of mass at the i th floor, V_{fx} and V_{fy} = reactive forces in horizontal x and y directions respectively and M_{fx} , M_{fy} and M_{fz} = reactive moments about the x -axis, y -axis and z -axis respectively from the soil medium.

On substitution of $\{\ddot{q}_i^x\}$ from Eq. (9), Eq. (11) becomes

$$[B]^T [M] \{\ddot{q}\} + [K_0'] \{\ddot{q}_0\} + \{P_f\} = -[K_1'] \{\ddot{q}_g\} \quad (12)$$

where $\{P_f\} = \{V_{fx} \ V_{fy} \ M_{fy} \ M_{fx} \ M_{fz}\}^T$ is a vector of reactive forces from the soil medium and $[K_0']$ and $[K_1']$ involve the terms $\sum_{i=0}^N m_i$, $\sum_{i=1}^N m_i h_i$, $\sum_{i=1}^N (-m_i y_{ci})$, $\sum_{i=0}^N I_{yi}$ and $\sum_{i=1}^N m_i h_i^2$, $\sum_{i=1}^N (-m_i y_{ci}) h_i$, $\sum_{i=1}^N m_i x_{ci}$, $\sum_{i=1}^N m_i x_{ci} h_i$, $\sum_{i=0}^N I_{zi}$ and $\sum_{i=1}^N m_i (y_{ci}^2 + x_{ci}^2)$ and $\sum_{i=0}^N I_{xi}$ and $\sum_{i=1}^N m_i h_i^2$. Details of these matrices are reported in Bhat (2004) and Appendix A.

In order to incorporate the compliance effect, use of frequency-dependent impedance functions is made. Frequency domain analysis, therefore, has been carried out first and response quantities then are transformed into the time domain using the Inverse Fast Fourier Transform IFFT technique.

3.3 Equations of motion in frequency domain

Equation (10) for the superstructure and Eq. (12) for the raft are converted into frequency domain by letting $\{\ddot{q}_g(t)\} = \{\bar{q}_g(\omega)\}e^{i\omega t}$ and any response quantity as $\bar{x} = x(\omega)e^{i\omega t}$ in which $\bar{x}(\omega)$ is the response quantity in frequency domain. The equations of motion in frequency domain are

$$\begin{aligned} (-\omega^2[M] + i\omega[C] + [K])\{\bar{q}(\omega)\} - \omega^2[M][B]\{\bar{q}_0(\omega)\} \\ = -[M][A]\{\bar{q}_g(\omega)\} \end{aligned} \quad (13)$$

$$\begin{aligned} \omega^2[B]^T[M]\{\bar{q}(\omega)\} - \omega^2[K'_0]\{\bar{q}_0(\omega)\} + \{\bar{P}_f(\omega)\} \\ = [K'_1]\{\bar{q}_g(\omega)\} \end{aligned} \quad (14)$$

When any of the quantities of $\{\bar{q}_g\} = 1$ and the other terms are equal to zero, the response quantity $\{\bar{x}\}$ is termed as the transfer function of the quantity.

The vector $\{\bar{P}_f\}$ can be obtained from $\{\bar{P}_f\} = [K''_0]\{q_0\}$, where $[K''_0]$ = the matrix of impedance functions.

In the present study frequency dependent impedance functions for rectangular footings resting on elastic half-space given by Wong and Luco [31] have been used.

3.4 Equations of motions in generalized coordinates

Let $\{\Phi\}$ be the normalized eigenvector of the superstructure fixed at base and the orthogonality conditions: $\{\Phi\}^T[M]\{\Phi\} = 1$, $\{\Phi\}^T[C]\{\Phi\} = 2\xi_n\omega_n$ and $\{\Phi\}^T[K]\{\Phi\} = \omega_n^2$ where, ω_n = a natural frequency of the fixed base structure and ξ_n = damping ratio in the n th mode of vibration.

Let $\{q(t)\} = \sum_{n=1}^j \Phi_n y_n$, in which, y_n = generalized coordinate in the n th mode and j = the number of mode shapes to be considered.

In the frequency domain this relation can be expressed as

$$\{\bar{q}(\omega)\} = \sum_{n=1}^j \Phi_n \bar{y}_n \quad (15)$$

On substitution of $\bar{q}(\omega)$ in Eq. (13) (for the superstructure) and making use of orthogonality conditions of mode shapes the Eq. (13) becomes

$$\begin{aligned} \bar{y}_n(\omega) \Upsilon_n - \omega^2 \{\Phi_n\}^T [M][B] \{\bar{q}_0(\omega)\} \\ = -\{\Phi_n\}^T [M][A] \{\bar{q}_g(\omega)\} \end{aligned} \quad (16)$$

where $\Upsilon_n = -\omega^2 + 2i\xi_n\omega\omega_n + \omega_n^2$

$$\begin{aligned} \bar{y}_n(\omega) = \frac{1}{\Upsilon_n} [\omega^2 \{\Phi_n\}^T [M][B] \{\bar{q}_0(\omega)\} \\ - \{\Phi_n\}^T [M][A] \{\bar{q}_g(\omega)\}] \end{aligned} \quad (17)$$

Similarly, using equations of motion for the foundation Eq. (14) and on substituting $\{\bar{q}(\omega)\}$ from Eq. (15), Eq. (17) become

$$\begin{aligned} \left[-\omega^2 [K'_0] + [K''_0] - \omega^4 \sum_{n=1}^j [D_n][D_n]^T \frac{1}{\gamma_n} \right] \{\bar{q}_0(\omega)\} \\ = - \left[[K'_1] + \omega^2 \sum_{n=1}^j [D_n][E_n]^T \frac{1}{\gamma_n} \right] \{\bar{q}_g(\omega)\} \end{aligned} \quad (18)$$

in which $[E_n] = [A]^T [M] \{\phi_n\}$, and $[K''_0]$ = the matrix of impedance functions and $[D_n] = [B]^T [M] \{\phi_n\}$,

The quantity $\{\bar{q}_0(\omega)\}$ can be obtained from Eq. 18 for each value of ω . $\bar{y}_n(\omega)$ is then obtained from Eq. (16) and $\bar{q}(\omega)$ from Eq. (15).

4. Numerical study

Various parameters influencing the response of symmetric multistorey buildings on compliant foundations due to torsional ground motion have been considered. These are: shear wave velocity V_s and angle of incidence θ , frequency ratio $\Omega = \omega_\theta/\omega_t$ (Ω = ratio of uncoupled fundamental torsional frequency, ω_θ to uncoupled fundamental translational frequency, ω_t) and uncoupled fundamental period of the building T in the direction of applied ground motion. O'Rourke *et al* [27] reported sites for which V_s is as low as 510 ft/s (155 m/s) and 590 ft/s (180 m/s) with the corresponding values of $\phi = 19.47^\circ$ and 13.93° (i.e. $\theta = 17.20^\circ$ and 12.21°) respectively. These values are based on the recorded earthquakes and shear wave velocity of the medium V_s obtained from the seventeen sites of the San Fernando Earthquake 1971. Higher angles of incidence are produced at hard soils with larger epicentral distances or shallow earthquakes [21]. In the present study shear wave velocity has been taken equal to 350 m/s, 250 m/s and 100m/s for the soils designated as firm soil, medium-firm soils and soft soil respectively. The values of θ adopted in the present study are $\theta = 5^\circ$, 10° and 20° . As higher angles of incidence have been reported for firm soils only therefore $\theta = 20^\circ$ has not been considered for soft soils cases. Similarly, the effect of lower values of θ , $\theta = 5^\circ$ for firm and medium-firm soil is very small [32], therefore $\theta = 10^\circ$ and 20° has only been considered in this study for these soils.

The methodology adopted in this study is presented in a flow chart as shown in figure 4. A symmetrical building plan comprising of frames as stiffening elements, shown in figure 5 is chosen for numerical study. Corresponding to this example building plan (EB) a set of six buildings are identified: EB[(T); (Ω)], in which T and Ω are the uncoupled fundamental period and frequency ratio of a building respectively. The buildings are supported on the raft with an aspect ratio $L/B=2.63$ (where L and B are the half lengths and breadths of the raft). The properties of the stiffening

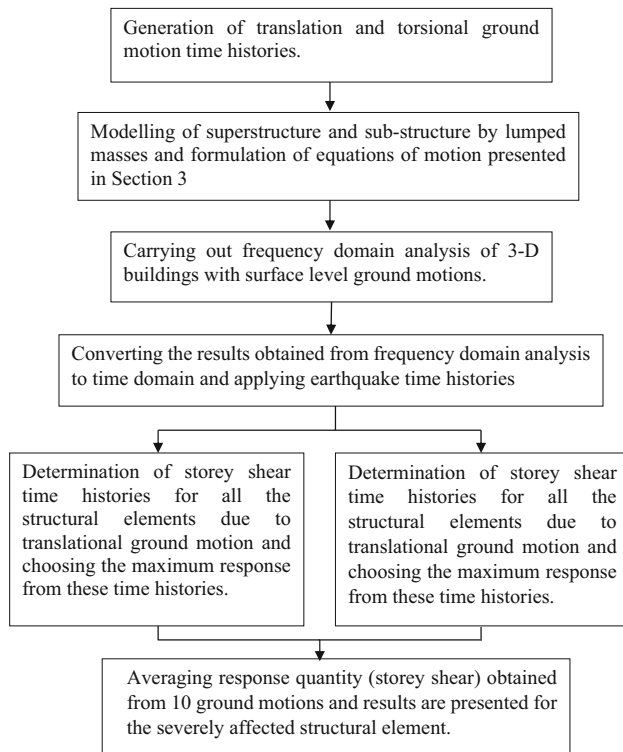


Figure 4. Flow chart showing methodology adopted in the study.

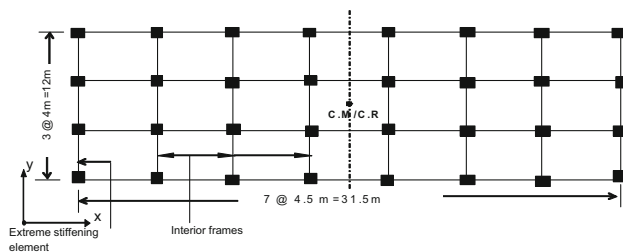


Figure 5. Example building plan (EB).

elements are assumed to be uniform along the height and the mass of each floor is assumed to be the same except at the top floor where it is assumed to be the 50% of the floor mass at other floors.

Framed buildings comprising of frames only as stiffening elements are considered in the present study. Floor slabs of these buildings are assumed to have infinite in-plane rigidity and no bending stiffness. Mass of each storey is lumped at the corresponding floor level. The properties of the structural elements are chosen to achieve the specific values of Ω and T . The frequency ratio Ω is chosen to be 0.65, 1.00 and 1.5 and the period of vibration T is chosen to be 0.3 s and 0.8 s. The chosen values of Ω cover practically the entire spectrum of torsionally flexible and torsionally stiff buildings. Similarly chosen values of T cover the low-rise frame buildings say up to 10 storeys. The values of T =

0.3 s and 0.8 s have been achieved by considering 3 and 10-storeyed buildings. The values of Ω are arrived at by an iterative process without changing the fundamental period T of the building in the direction of applied ground motion. For four buildings (Example Building plans) EB[(0.3, 0.8); (1.0, 1.5)] corresponding to T = 0.3 s and 0.8 s with Ω = 1.0 and 1.5. For example, EB[(0.3); (1.0)], and EB[(0.3); (1.5)] represent the example buildings having period of vibration of 0.3s and frequency ratios Ω = 1.0 and 1.5 respectively. The specified values of pairs of Ω = (1.0, 1.5) and T = (0.3, 0.8) are arrived at by changing the properties of columns in an iterative manner. Similarly, for the remaining two buildings EB[(0.3, 0.8); (0.65)], the specified values of pairs of Ω = 0.65 and T = (0.3, 0.8) are arrived at by changing the properties of the columns and also by changing the polar mass moment of inertia of floors.

In order to incorporate SSI effects, frequency-dependent impedance functions for rectangular footings resting on elastic half-space have been obtained from the charts and tables of [33]. These impedance functions have been modified to incorporate the soil hysteretic damping (β) by adding material dashpot constant ($2K\beta/\omega$, K is dynamic stiffness of footing) to the radiation damping constant C [34]. The value of soil hysteretic damping has been taken as 7.5%. The impedance functions for the aspect ratio $L/B=2.63$ have been interpolated from $L/B = 2.0$ and $L/B = 3.0$ for different soil conditions (firm soil, medium-firm soil and soft soil).

Ten translational ground motion histories and corresponding ten torsional ground motion histories have been generated based on the equations presented in section 2. The analysis has been carried out using softwares prepared at IIT Delhi.

In the present study, translational ground motion histories are generated with $pga = 0.1g$, earthquake duration = 20.48 s and time interval = 0.02 s. The translational ground motion histories have been generated by assigning phase angle Φ_j random values in Eq. (6). Corresponding to these translational ground motion histories, torsional ground motion histories for each shear wave velocity V_s ($V_s = 250$ m/s, 350 m/s and 100m/s) and angle of incidence θ ($\theta = 5^\circ$, 10° and 20°) are further generated. A typical set of ground motion histories is shown in figure 6. The translational ground motion is assumed to act in y -direction only.

5. Results and discussions

Analysis has been carried out for all the buildings reported in the previous section subjected to translational ground motion and simultaneously acting translational and torsional ground motions. Storey shear time histories $V(t)$ produced due to translational ground motion and simultaneously acting translational and torsional ground motion are obtained. Typical plots of base shear time histories

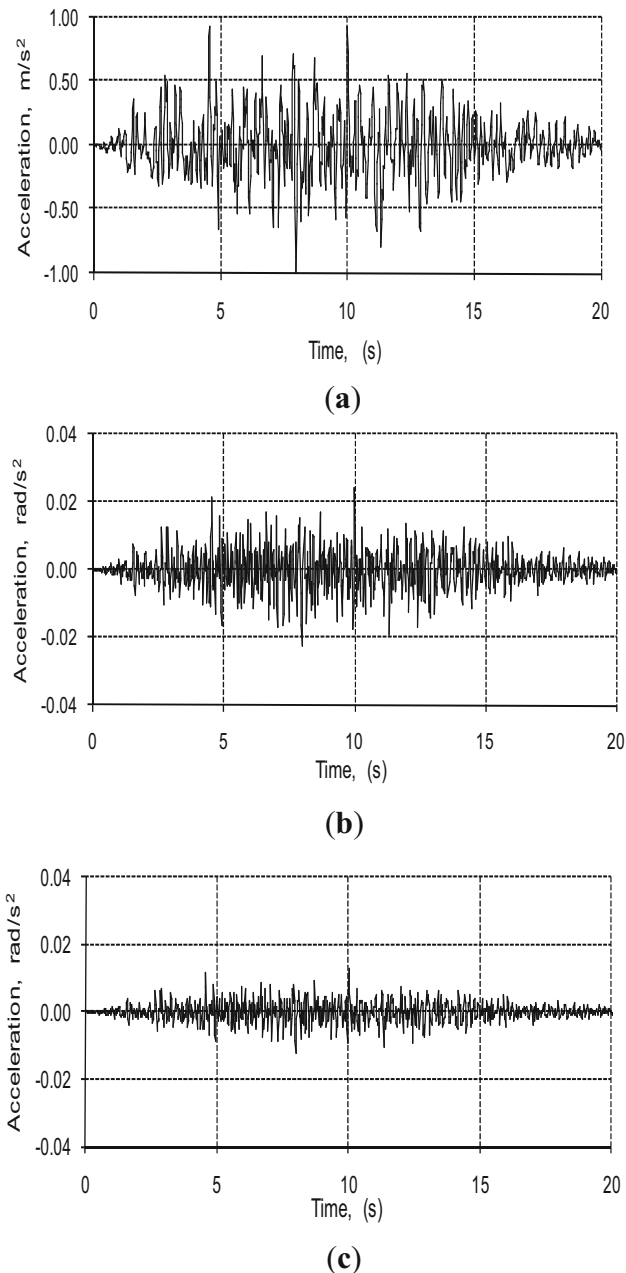


Figure 6. Ground motion time histories for firm soil case: (a) translational ground motion, (b) torsional ground motion, $\theta = 20^\circ$ and (c) torsional ground motion, $\theta = 10^\circ$.

$V_{t,f}(t)$, $V_{r,f}(t)$ and $V_{c,f}(t)$ for the extreme stiffening element (stiffening element at the extreme edge) of one of the buildings EB[(0.3); (1.0)] with the fixed base foundation on firm soil are shown in figure 7, (the subscripts t , r and c for $V(t)$ or any other quantity stand for translational ground motion, torsional ground motion and combined translational and torsional ground motions respectively and subscript f stands for fixed base foundation). Similarly, base shear time histories $V_{t,i}(t)$, $V_{r,i}(t)$ and $V_{c,i}(t)$ (subscript i refers to the soil-structure interaction (SSI) effects) for the

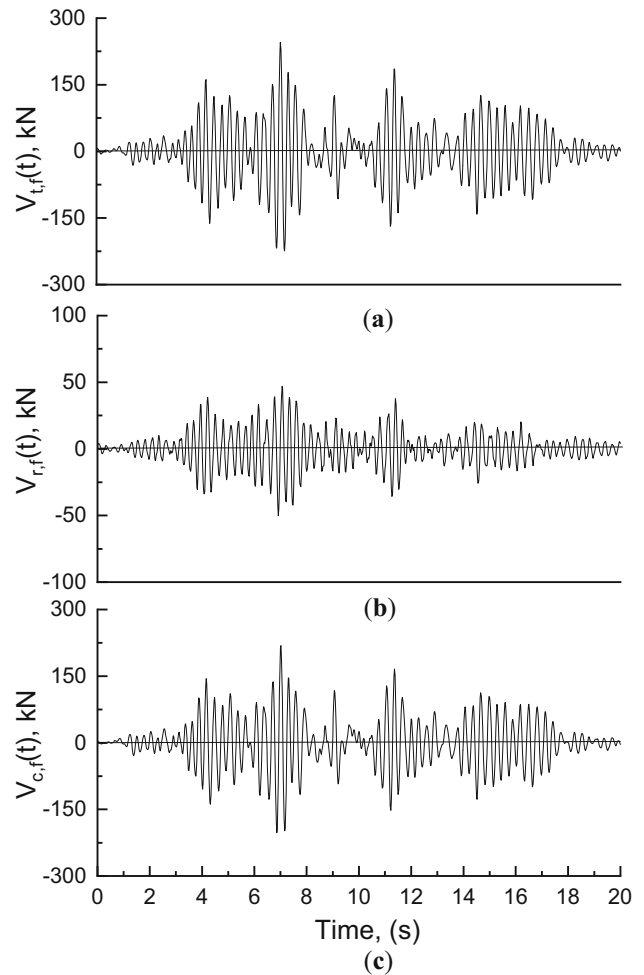


Figure 7. Base shear time history for the stiffening element at the extreme edge of EB[(0.3); (1.0)] on firm soil due to: (a) translation, (b) torsion and (c) translation and torsion ($\theta = 20^\circ$, fixed foundation).

stiffening element at the extreme edge of the same building and on the same soil incorporating SSI effects are shown in figure 8. These base shear time histories are due to a sample ground motion on firm soil and $\theta = 20^\circ$. From these figures, it may be noted that the peak base shears due to translational and torsional ground motions do not occur at the same time instants. In the present case, the peak shear due to simultaneously acting translational and torsional ground motion occurs at a time instant when peak shear due to translational ground motion occurs. The absolute peak storey shears $|V_{t,f}|$, $|V_{c,f}|$, $|V_{t,i}|$ and $|V_{c,i}|$, are of design interest and are obtained from such plots of $V(t)$. These absolute values of shears have been evaluated for ten ground motion histories and average values of these shears are used in the present study. The results for the extreme stiffening element for which the effect of torsional ground motion would be the maximum are presented.

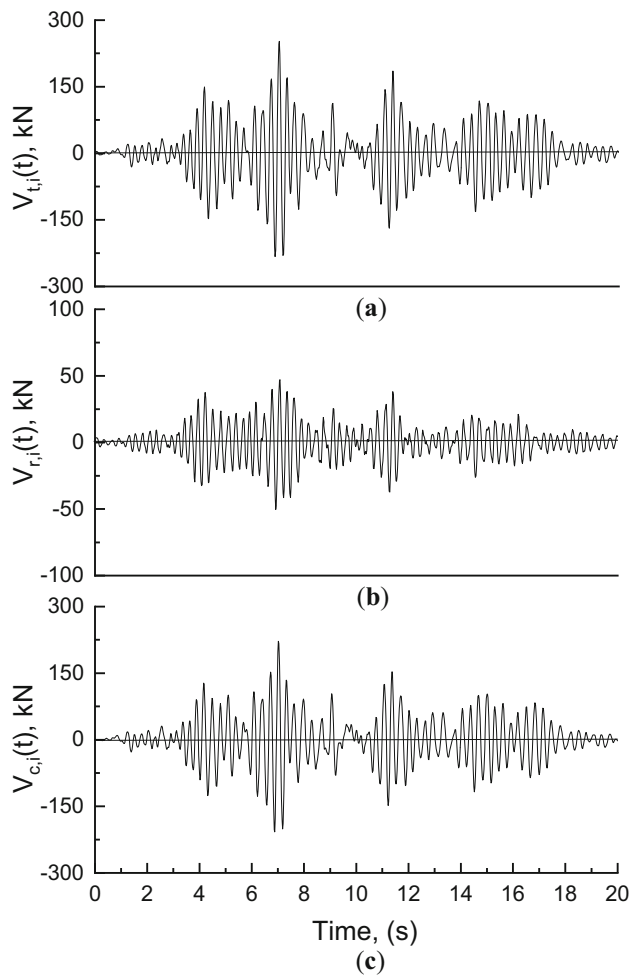


Figure 8. Base shear time history for the stiffening element at the extreme edge of EB[(0.3); (1.0)] on firm soil due to: (a) translation (b) torsion and (c) translation and torsion ($\theta = 20^\circ$, compliant foundation).

In the present study, the ratio $\frac{|V_{t,d}|}{|V_{t,f}|} = R_{ti,tf}$ indicates the compliance effects on the storey shears when subjected to translation ground motion only, the ratio $\frac{|V_{c,f}|}{|V_{t,f}|} = R_{cf,tf}$ indicates the effect of torsional ground motion and the ratio $\frac{|V_{c,d}|}{|V_{t,f}|} = R_{ci,tf}$ indicates the effect of both SSI and torsional ground motion. These ratios are of design interest. A value of these ratios ($R_{ti,tf}$, $R_{cf,tf}$ and $R_{ci,tf}$) greater than one indicates an increase in storey shears and a value lesser than one indicates a decrease in storey shears.

The effect of soil-structure interaction on base shear due to translational ground motion, $R_{ti,tf}$ for extreme stiffening element is shown in table 1. It is observed that the SSI effects are generally small for the buildings considered i.e., in the period range of 0.3s to 0.8s. For low period buildings, EB[(0.3); (0.65, 1.0, 1.5)] on soft soil the ratio $R_{ti,tf}$ in storey 1 (base shear) is 0.90 i.e. 10% reduction in base

shear. However, for high period buildings, EB[(0.8); (0.65, 1.0, 1.5)] on medium-firm soil, there is an increase in base shear up to 6% owing to particular characteristics of the transfer function of base shear for this building and psdf of ground motion [32].

Now consider the effect of torsional ground motion on base shear, $R_{cf,tf}$, for extreme stiffening element (table 2). From this table, it is observed that for torsionally stiff buildings with $T = 0.3s$, EB[(0.3); (1.5)] the effect of torsional ground motion is small and for buildings with $T = 0.8s$, EB[(0.8); (1.5)] this effect is negligible, for all soil types with all θ . For torsionally flexible buildings with $T = 0.3s$, EB[(0.3); (0.65)], the increase in base shear due to torsional ground motion for the extreme stiffening element is about 18% ($R_{cf,tf} = 1.18$) for medium-firm soil with $\theta = 20^\circ$, and about 36% ($R_{cf,tf} = 1.36$) for soft soil with $\theta = 10^\circ$. However, for these buildings with $T = 0.8s$, EB[(0.8); (0.65)], this increase is about 8% for medium-firm soils and about 10% for soft soil with $\theta = 10^\circ$. Similarly for torsionally medium stiff buildings with $T = 0.3s$, EB[(0.3); (1.0)], the increase in base shear is up to 15% for medium-

Table 1. Effect of SSI on base shear due to translational ground motion ($R_{ti,tf}$) for buildings EB[(0.3), (0.8); (0.65), (1.0), (1.5)]

Period (s)	Soil type	Frequency ratio (Ω)		
		1.5	1.0	0.65
0.3	Firm soil	0.96	0.96	0.96
	Medium-firm soil	0.98	0.98	0.98
	Soft soil	0.90	0.90	0.90
0.8	Firm soil	1.00	1.00	1.00
	Medium-firm soil	1.06	1.06	1.06
	Soft soil	0.93	0.93	0.93

Table 2. Effect of torsional ground motion on base shear ($R_{cf,tf}$) for buildings EB[(0.3), (0.8); (0.65), (1.0), (1.5)]

Period (s)	Soil type	θ	Frequency ratio (Ω)		
			1.5	1.0	0.65
0.3	Firm soil	20°	1.06	1.12	1.14
	Medium-firm soil		1.04	1.15	1.18
	Soft soil		–	–	–
	Firm soil	10°	1.06	1.06	1.08
	Medium-firm soil		1.02	1.07	1.06
	Soft soil		1.09	1.18	1.36
0.8	Soft soil	5°	1.04	1.08	1.15
	Firm soil	20°	1.05	1.05	1.06
	Medium-firm soil		1.06	1.06	1.09
	Soft soil		–	–	–
	Firm soil	10°	1.02	1.03	1.04
	Medium-firm soil		1.02	1.03	1.05
	Soft soil		1.04	1.06	1.10
	Soft soil	5°	1.02	1.03	1.05

firm soil with $\theta = 20^\circ$. For these buildings with $T = 0.8s$, this increase in base shear is small ($R_{cf, tf} = 1.05$) for all buildings for all soil cases with all θ .

Similarly, now consider the effect of torsional ground motion with SSI on base shear, $R_{ci, tf}$ (table 3). Two mutually opposing phenomena may be identified: (i) due to the SSI effect the base shear is generally reduced as observed in $R_{ti, tf}$ (table 1), and (ii) due to the incorporation of torsional ground motion there is an increase in these shears as observed in $R_{cf, tf}$ (table 2). For torsionally stiff buildings, EB[(0.3), (0.8); (1.5)] net effect of both torsional ground motion and soil-structure interaction is negligible

Table 3. Effect of SSI and torsional ground motion on base shear ($R_{ci, tf}$) for buildings EB[(0.3), (0.8); (0.65), (1.0), (1.5)]

Period (s)	Soil type	θ	Frequency ratio (Ω)			
			1.5	1.0	0.65	
0.3	Firm soil	20°	1.06	1.12	1.12	
	Medium-firm soil		1.01	1.14	1.22	
	Soft soil		–	–	–	
	Firm soil	10°	1.01	1.05	1.07	
	Medium-firm soil		0.99	1.05	1.07	
	Soft soil		0.96	0.99	1.34	
0.8	Soft soil	5°	0.93	0.94	1.12	
	Firm soil		20°	1.05	1.06	1.07
	Medium-firm soil			1.07	1.12	1.15
	Soft soil	–		–	–	
	Firm soil	10°	1.02	1.03	1.04	
	Medium-firm soil		1.06	1.09	1.11	
	Soft soil		0.93	0.98	1.05	
	Soft soil	5°	0.93	0.96	1.05	

for all soil types with all θ . However, for torsionally flexible buildings with $T = 0.3s$, EB[(0.3); (0.65)], increase in base shear for the extreme stiffening element is about 22% ($R_{ci, tf} = 1.22$) as compared to $R_{cf, tf} = 1.18$ (18%) for medium-firm soil with $\theta = 20^\circ$. This value is about 34% ($R_{ci, tf} = 1.34$) as compared to $R_{cf, tf} = 1.36$ (36%) for soft soil with $\theta = 10^\circ$. However, for these buildings with $T = 0.8s$, EB[(0.8); (0.65)], the increase in base shear is 14% as compared to $R_{cf, tf} = 1.08$ (8%) for medium-firm soil with $\theta = 20^\circ$ and about 6% ($R_{ci, tf} = 1.06$) as compared to $R_{cf, tf} = 1.10$ (10%) for soft soil with $\theta = 10^\circ$ (tables 2 and 3). For torsionally medium stiff buildings with $T = 0.3s$, EB[(0.3); (1.0)], the increase in base shear is up to 14% ($R_{ci, tf} = 1.14$) as compared to $R_{cf, tf} = 1.15$ (15%) for medium-firm soil with $\theta = 20^\circ$ and for these medium range torsionally stiff buildings with $T = 0.8s$, EB[(0.8); (1.0)] the increase in base shear is about 10% ($R_{ci, tf} = 1.10$) as compared to $R_{cf, tf} = 1.05$ (5%), (tables 2 and 3).

The reason for increase in the base shears of these buildings is dependent on the characteristics of the fundamental frequency of the buildings and the spectral power of the earthquake corresponding to that frequency, as fundamental frequency of the building is mainly responsible for the overall response. Tables 4 and 5 show the fundamental frequencies of the spectrum buildings considered. From these tables it is seen that for buildings EB[(0.3); (0.65, 1.0, 1.5)], and EB[(0.8); (0.65, 1.0, 1.5)] the torsional frequencies (ω_θ) are in the range of 12-30 rad/s and 5-11 rad/s respectively. Corresponding to these frequencies the maximum spectral power of torsional ground motion (psdf of torsional ground motion) is for soft soil (figure 1b) followed by medium-firm soil and firm soil. The maximum spectral power of ground motion in soft soil corresponding to the

Table 4. Fundamental frequencies for EB[(0.3); (0.65, 1.0, 1.5)] with soil type

Ω	Fixed case		Compliant case					
			Firm soil		Medium firm soil		Soft soil	
	ω_{tf}	ω_{0f}	ω_{ti}	$\omega_{\theta i}$	ω_{ti}	$\omega_{\theta i}$	ω_{ti}	$\omega_{\theta i}$
0.65	20.95	13.86	20.25	13.81	19.94	13.5	15.95	12.27
1	20.95	22.3	20.25	22.09	19.94	21.78	15.95	19.94
1.5	20.95	30.1	20.25	29.45	19.94	28.84	15.95	25.5

Table 5. Variation of fundamental frequencies for EB[(0.8); (0.65, 1.0, 1.5)] with soil type

Ω	Fixed case		Compliant case					
			Firm soil		Medium firm soil		Soft soil	
	ω_{tf}	ω_{0f}	ω_{ti}	$\omega_{\theta i}$	ω_{ti}	$\omega_{\theta i}$	ω_{ti}	$\omega_{\theta i}$
0.65	7.98	5.22	7.06	5.22	6.75	5.22	4.29	4.91
1	7.98	8.28	7.06	8.28	6.75	8.28	4.29	7.67
1.5	7.98	11.35	7.06	11.35	6.75	11.35	4.29	9.82

fundamental torsional frequencies of the buildings is responsible for higher response. However, for EB[(0.8)], the response due to translational ground motion (figure 1a) is high corresponding to $\omega_t = 4\text{--}8$ rad/s, for soft soil case which leads to a lower relative response due to torsional ground motion as compared to EB[(0.3)] buildings.

From the above results, it is observed that the effect of torsional ground motion on base shear is significant for torsionally flexible buildings with low period ($T=0.3\text{s}$) for medium-firm soil and soft soil with high values of θ . Further, it is observed that the SSI effect on base shear is small for all the buildings for all soil cases and all θ .

Now consider the variation of ratios ($R_{ti,tf}$, $R_{cf,tf}$ and $R_{ci,tf}$) along the height. The variation of these ratios $R_{ti,tf}$, $R_{cf,tf}$ and $R_{ci,tf}$ along the height with storey number for the extreme stiffening element for all the buildings are shown in figures 9, 10, 11, 12, 13, 14, 15, 16, 17, 18, 19, 20, 21 and 22. The quantities of absolute shear are constant in a storey; therefore, these ratios are also constant in a storey. A

parameter, σ similar to standard deviation is identified, $\sigma =$

$\sqrt{\frac{\sum_{j=1}^N (R_j - R_b)^2}{N}}$ which is a measure of the deviation of storey shears along the height from the base shear, where R indicates the values of ratios $R_{ti,tf}$, $R_{cf,tf}$ and $R_{ci,tf}$ identified above and the subscript j and b indicate j th storey and ground storey respectively. The deviation, σ of $R_{ti,tf}$, $R_{cf,tf}$ and $R_{ci,tf}$ are shown in tables: 6, 7 and 8. In general, variations in the ranges: $0 < \sigma < 0.025$; $0.025 < \sigma < 0.05$ and $\sigma > 0.05$ are taken to be very small, small and significant respectively.

The variation of $R_{ti,tf}$ along the height for extreme stiffening element of all the buildings EB[(0.3, 0.8); (0.65, 1.0, 1.5)] for all soil cases, is small or very small except for the buildings EB[(0.8); (0.65, 1.0, 1.5)] where the variation is significant for the soft soil case (figures 9 and 10 and table 6). $R_{ti,tf}$ varies from 0.93 at the base to 1.11 at the top (i.e., storey shear is reduced by 7% in the bottommost storey; however, there is an increase of 11% in the top storey when SSI is also incorporated).

Similarly, the variation of $R_{cf,tf}$ along the height for extreme stiffening element of all the buildings EB[(0.3, 0.8); (0.65, 1.0, 1.5)] for all soil cases is also small or very small except for the building EB[(0.8); (0.65)] for the medium-firm soil case with $\theta = 20^\circ$ where the variation is significant (figures 11, 12, 13, 14, 15, 16 and table 7). $R_{cf,tf}$ varies from 1.09 at the base to 1.20 at top (i.e., storey shear is increased by 9% in the bottommost storey and by 20% in the top storey when torsional ground motion is also considered).

From the above results, it is observed that the effect of SSI (translation case only) and torsional ground motion (without SSI) on storey shear along the height generally nearly remains the same, however, in some cases, the effect on storey shears vary significantly.

The variation of $R_{ci,tf}$ (i.e. when the combined effect of torsional ground motion and SSI is considered) along the height for extreme stiffening element is small for buildings with $T = 0.3\text{s}$, EB[(0.3); (0.65), (1.0), (1.5)] for all soil cases with all θ , except for building EB[(0.3); (1.5)] for firm and medium-firm soil cases, where the variation is very small (figures 17, 18, 19 and table 8). However, for buildings with $T=0.8\text{s}$, the variation of $R_{ci,tf}$ along the height for extreme stiffening element is significant for almost all buildings, EB[(0.8); (0.65), (1.0), (1.5)] for all soil cases with all θ , (figures 20, 21, 22 and table 8). $R_{ci,tf}$ varies from 1.08 at the base to 1.21 at the top (i.e., storey shear is increased by 8%

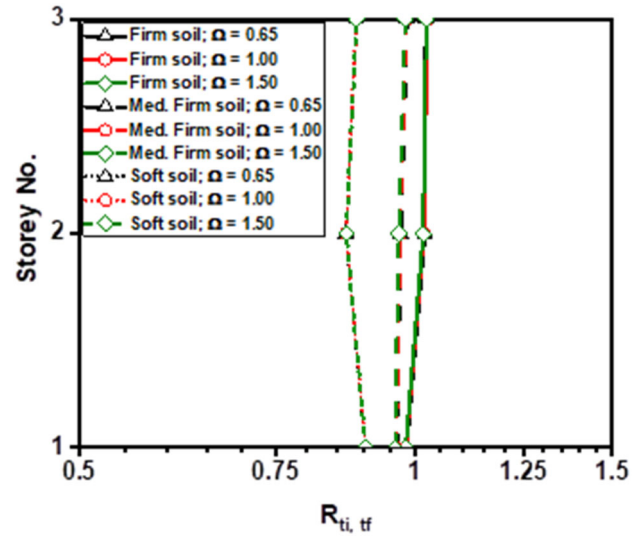


Figure 9. Variation of $R_{ti,tf}$ along height for extreme stiffening element of EB[(0.3); (0.65, 1.0, 1.5)] on: firm soil, medium-firm soil and soft soil.

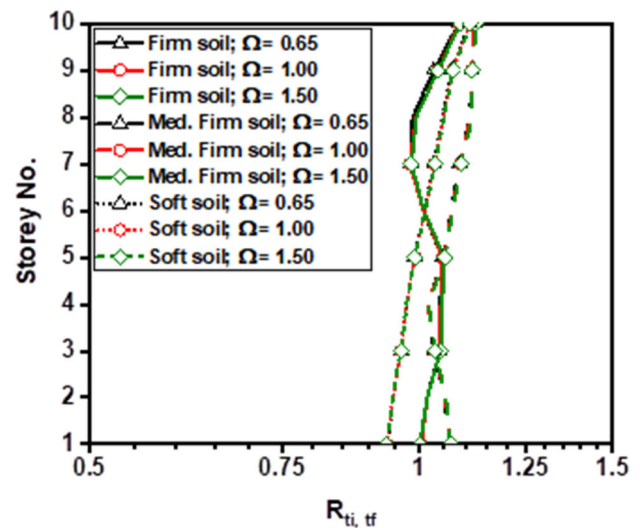


Figure 10. Variation of $R_{ti,tf}$ along height for extreme stiffening element of EB[(0.8); (0.65, 1.0, 1.5)] on: firm soil, medium-firm soil and soft soil.

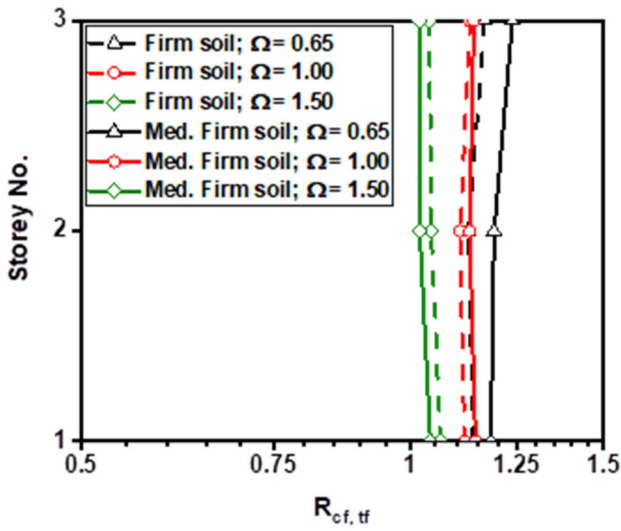


Figure 11. Variation of $R_{cf,tf}$ with different soil types for $\theta = 20^\circ$ for the stiffening element at the extreme edge of EB[(0.3)].

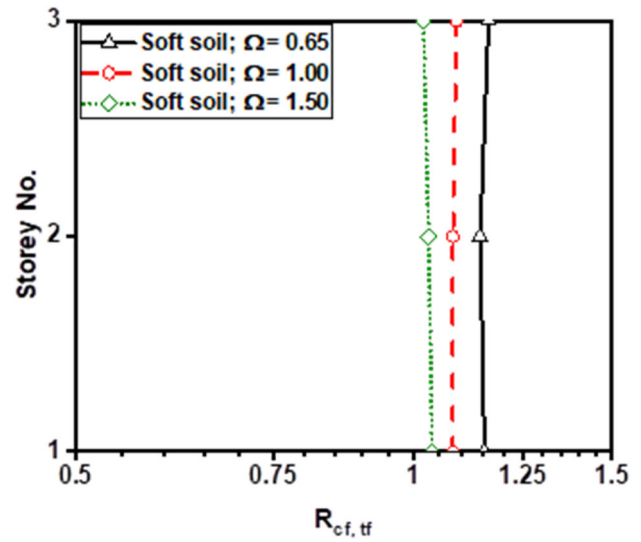


Figure 13. Variation of $R_{cf,tf}$ with Ω for soft soil and $\theta = 5^\circ$ for the stiffening element at the extreme edge of EB[(0.3)].

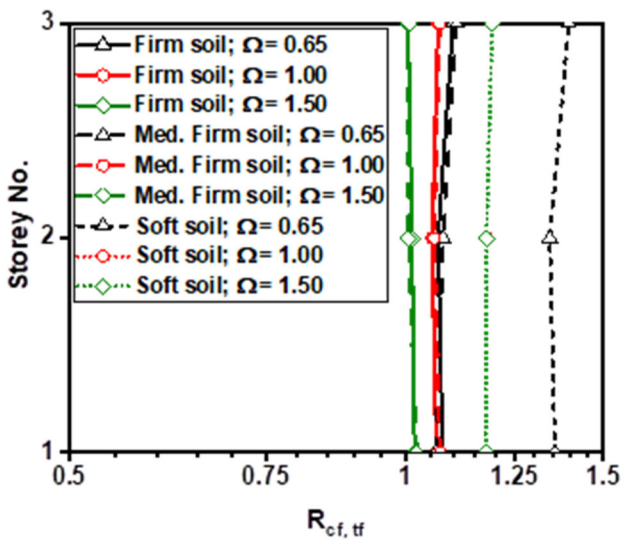


Figure 12. Variation of $R_{cf,tf}$ with different soil types for $\theta = 10^\circ$ for the stiffening element at the extreme edge of EB[(0.3)].

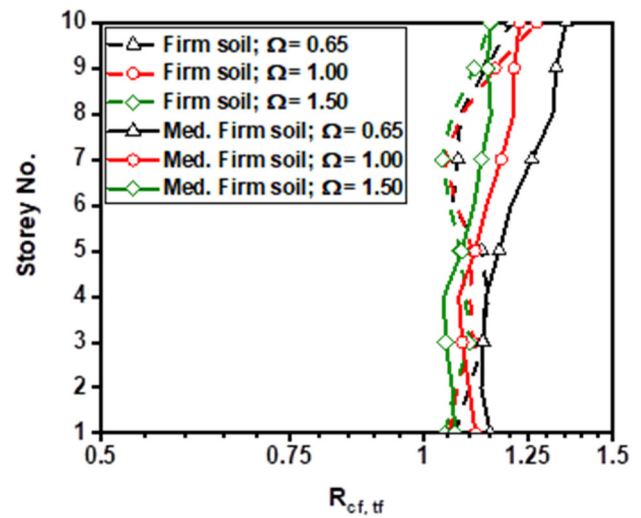


Figure 14. Variation of $R_{cf,tf}$ with different soil types for $\theta = 20^\circ$ for the stiffening element at the extreme edge of EB[(0.8)].

and 21% in the bottommost storey and in the top storey, respectively) for building EB[(0.8); (0.65)] for medium-firm soil with $\theta = 20^\circ$. Similarly $R_{ci,tf}$ varies from 0.98 at the base to 1.17 at the top (i.e., storey shear is reduced by 2% in the bottommost storey, however, there is an increase of 17% in the top storey). Also, $R_{ci,tf}$ varies from 0.93 at the base to 1.11 at the top (i.e. storey shear is reduced by 7% in the bottommost storey, however, there is an increase of 11% in the top storey). The increase in top storey shear is

18% for EB[(0.8); (1.0)] and EB[(0.8); (1.5)], respectively, for soft soil with $\theta = 10^\circ$.

Thus, from the results in the above paragraph, it is observed that the combined effect of torsional ground motion and SSI on the distribution of storey shears along the height nearly remains the same for buildings with low period ($T=0.3s$) but varies significantly for high period buildings ($T=0.8s$). This variation in the distribution of storey shears along the height in the case of EB[(0.8)] buildings is attributed to the contribution of higher modes in the response quantity.

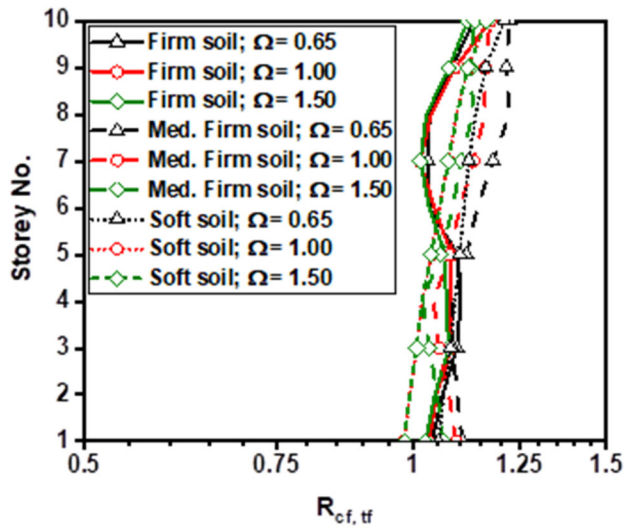


Figure 15. Variation of $R_{cf,tf}$ with different soil types for $\theta = 10^\circ$ for the stiffening element at the extreme edge of EB[(0.8)].

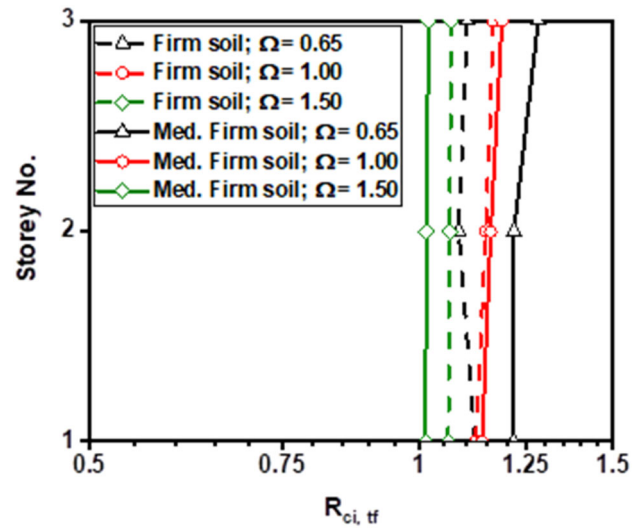


Figure 17. Variation of $R_{ci,tf}$ with different soil types for $\theta = 20^\circ$, for the stiffening element at the extreme edge of EB[(0.3)].

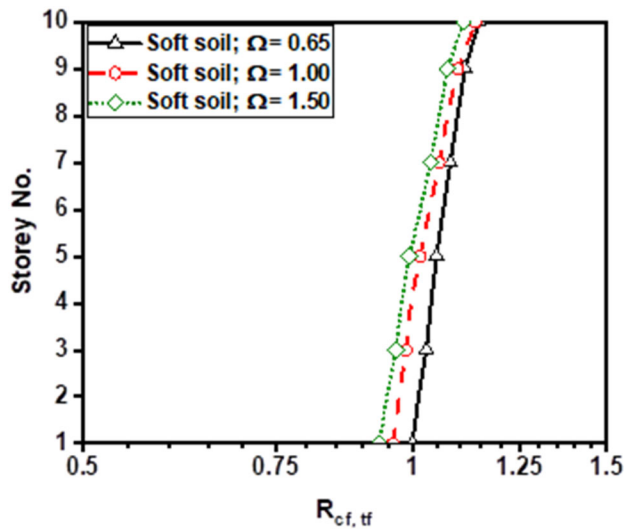


Figure 16. Variation of $R_{cf,tf}$ with Ω for soft soil and $\theta = 5^\circ$ for the stiffening element at the extreme edge of EB[(0.3)].

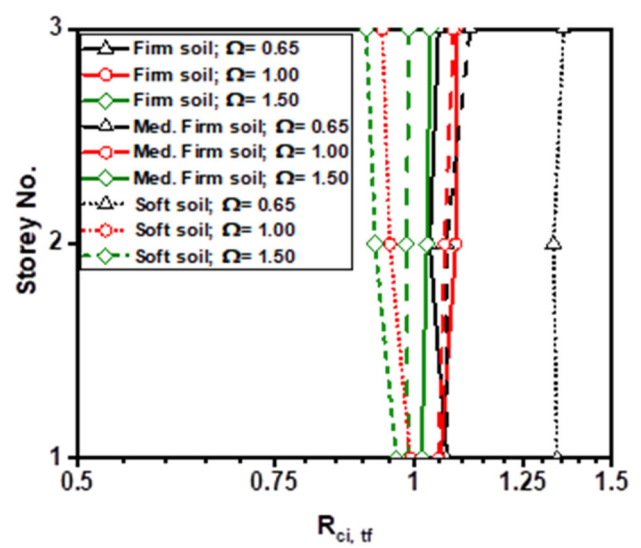


Figure 18. Variation of $R_{ci,tf}$ with different soil types for $\theta = 10^\circ$, for the stiffening element at the extreme edge of EB[(0.3)].

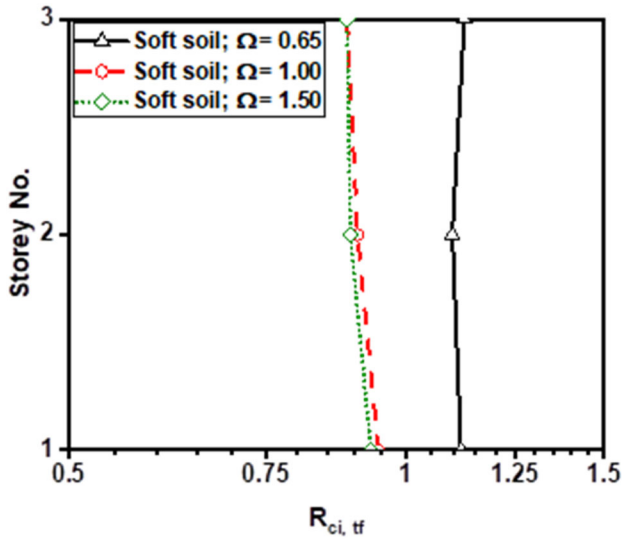


Figure 19. Variation of $R_{ci,tf}$ with Ω for soft soil and $\theta = 5^\circ$ for the stiffening element at the extreme edge of EB[(0.3)].

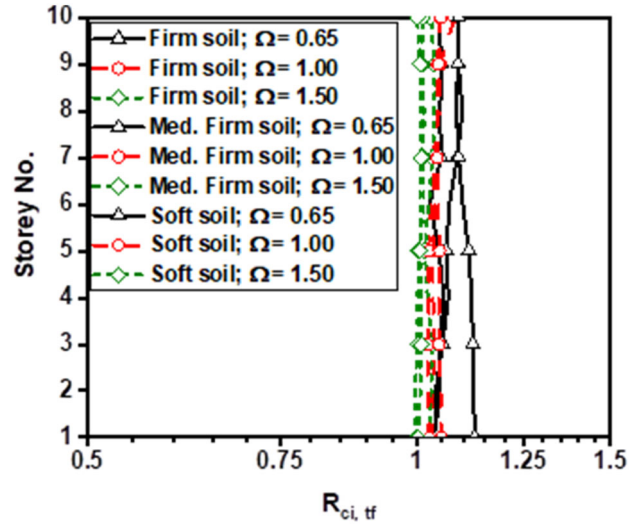


Figure 21. Variation of $R_{ci,tf}$ with different soil types for $\theta = 10^\circ$, for the stiffening element at the extreme edge of EB[(0.8)].

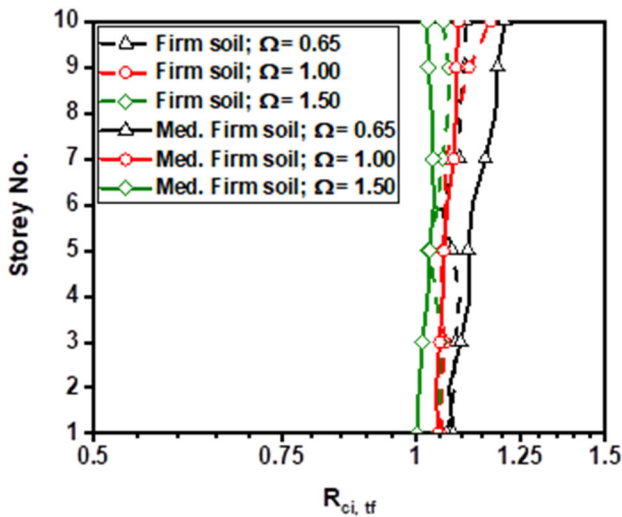


Figure 20. Variation of $R_{ci,tf}$ with different soil types for $\theta = 20^\circ$, for the stiffening element at the extreme edge of EB[(0.8)].

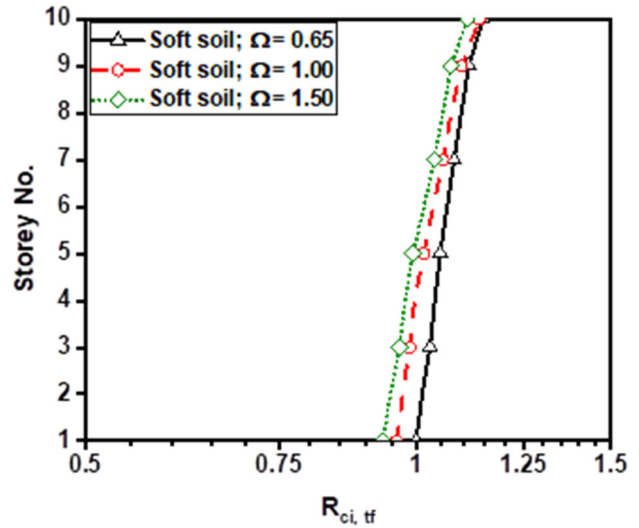


Figure 22. Variation of $R_{ci,tf}$ with Ω for soft soil and $\theta = 5^\circ$ for the stiffening element at the extreme edge of EB[(0.8)].

Table 6. Deviation, σ of $R_{i,tf}$ for buildings EB[(0.3), (0.8); (0.65, 1.0, 1.5)]

Building	Soil type		
	Firm soil	Medium-firm soil	Soft soil
EB[(0.3); (0.65, 1.0, 1.5)]	0.032	0.012	0.022
EB[(0.8); (0.65, 1.0, 1.5)]	0.039	0.035	0.092

Table 7. Deviation, σ of $R_{cf,tf}$ for buildings EB[(0.3), (0.8); (0.65, 1.0, 1.5)]

Soil Type	θ	Buildings EB[(0.3); (0.65, 1.0, 1.5)]			Buildings EB[(0.8); (0.65, 1.0, 1.5)]		
		$\Omega = 0.65$	$\Omega = 1.0$	$\Omega = 1.5$	$\Omega = 0.65$	$\Omega = 1.0$	$\Omega = 1.5$
Firm soil	20°	0.017	0.009	0.019	0.028	0.028	0.029
Medium-firm soil	20°	0.032	0.009	0.020	0.060	0.023	0.034
Firm soil	10°	0.015	0.006	0.009	0.012	0.009	0.015
Medium-firm soil	10°	0.028	0.007	0.014	0.026	0.009	0.022
Soft soil	10°	0.024	0.009	0.028	0.018	0.009	0.023
Soft soil	5°	0.008	0.004	0.012	0.008	0.005	0.011

Table 8. Deviation, σ of $R_{ci,tf}$ for buildings EB[(0.3), (0.8); (0.65, 1.0, 1.5)]

Soil Type	θ	Buildings EB[(0.3); (0.65, 1.0, 1.5)]			Buildings EB[(0.8); (0.65, 1.0, 1.5)]		
		$\Omega = 0.65$	$\Omega = 1.0$	$\Omega = 1.5$	$\Omega = 0.65$	$\Omega = 1.0$	$\Omega = 1.5$
Firm soil	20°	0.024	0.028	0.005	0.063	0.083	0.050
Medium-firm soil	20°	0.037	0.031	0.004	0.107	0.062	0.053
Firm soil	10°	0.024	0.028	0.012	0.047	0.056	0.044
Medium-firm soil	10°	0.031	0.020	0.002	0.068	0.047	0.044
Soft soil	10°	0.012	0.040	0.041	0.075	0.093	0.097
Soft soil	5°	0.012	0.041	0.034	0.079	0.093	0.097

6. Conclusions

From the results obtained by analyzing three types of buildings (torsionally flexible, torsionally medium stiff and torsionally stiff) of periods of vibration 0.3 s and 0.8 s (low period and high period) on three types of soil medium (firm, medium firm and soft), the following conclusions are drawn.

- a. Effect of torsional ground motion on storey shears is significant in the case of torsionally flexible buildings with low periods of vibration on soft soils and medium-firm soil. The increase in base shear for the extreme stiffening element for buildings considered is up to 35% and about 20% for low period buildings on soft soil and medium-firm soil, respectively. The provision for incorporation of torsional ground motion in seismic codes in the form of accidental eccentricity needs to be looked into for such types of buildings.
- b. The distribution of storey shears along the height varies significantly for high period buildings ($T = 0.8$ s), when torsional ground motion and SSI effects are considered.

- c. Effect of SSI including torsional ground motion on base shear is small for all the buildings for all soil types. Similar effect is generally observed in the case of translational ground motion also.

Appendix A

Equation of motion for the raft

The equations of equilibrium of the raft are provided in equations 11(a) to 11(e). On substitution of \ddot{q}_i^r from Eq. 8, Eqs. 11(a) to 11(e) become:

Translation along x-direction:

$$\begin{aligned}
 &\ddot{q}_{ox} \sum_{i=1}^N m_i + \ddot{q}_{gx} \sum_{i=0}^N m_i + \sum_{i=1}^N m_i \ddot{q}_i + \ddot{q}_{\theta z} \sum_{i=1}^N (-m_i y_{ci}) \\
 &+ \ddot{\theta}_y \sum_{i=1}^N h_i m_i + \ddot{\theta}_z \sum_{i=1}^N (-m_i y_{ci}) \\
 &+ \sum_{i=1}^N (-m_i y_{ci} \ddot{q}_{2N+i}) + V_{fx} = 0 \tag{A1a}
 \end{aligned}$$

Rotation about y-axis:

$$\begin{aligned} \ddot{q}_{0x} \sum_{i=1}^N m_i h_i + \ddot{q}_{gx} \sum_{i=0}^N m_i h_i + \sum_{i=1}^N m_i h_i \ddot{q}_i + \ddot{\theta}_y \sum_{i=1}^N h_i^2 m_i \\ + \ddot{q}_{0z} \sum_{i=1}^N (-m_i y_{ci}) h_i + \ddot{\theta}_z \sum_{i=1}^N (-m_i y_{ci}) h_i \\ + \sum_{i=1}^N (-m_i y_{ci} h_i) \ddot{q}_{2N+i} + \ddot{\theta}_y \sum_{i=0}^N I_{yi} + M_{fy} = 0 \end{aligned} \tag{A1b}$$

Translation along y-direction:

$$\begin{aligned} \ddot{q}_{0y} \sum_{i=1}^N m_i + \ddot{q}_{gy} \sum_{i=0}^N m_i + \sum_{i=1}^N m_i \ddot{q}_{N+i} + \ddot{q}_{0z} \sum_{i=1}^N m_i x_{ci} \\ + \ddot{\theta}_x \sum_{i=1}^N m_i h_i + \ddot{\theta}_z \sum_{i=1}^N m_i x_{ci} + \sum_{i=1}^N m_i x_{ci} \ddot{q}_{2N+i} + V_{fy} \\ = 0 \end{aligned} \tag{A1c}$$

Rotation about x-axis:

$$\begin{aligned} \ddot{q}_{0y} \sum_{i=1}^N m_i h_i + \ddot{q}_{gy} \sum_{i=0}^N m_i h_i + \sum_{i=1}^N m_i \ddot{q}_{N+i} h_i \\ + \ddot{\theta}_x \sum_{i=1}^N h_i^2 m_i + \ddot{q}_{0z} \sum_{i=1}^N m_i x_{ci} h_i \\ + \ddot{\theta}_z \sum_{i=1}^N m_i x_{ci} h_i + \sum_{i=1}^N (m_i x_{ci} \ddot{q}_{2N+i}) h_i \\ + \ddot{\theta}_x \sum_{i=0}^N I_{xi} + M_{fx} = 0 \end{aligned} \tag{A1d}$$

Rotation about z-axis:

$$\begin{aligned} \sum_{i=1}^N m_i (-y_{ci} \ddot{q}_{0x} + x_{ci} \ddot{q}_{0y}) + \sum_{i=1}^N m_i h_i (-y_{ci} \ddot{\theta}_y + x_{ci} \ddot{\theta}_x) \\ + \sum_{i=1}^N m_i (-y_{ci} \ddot{q}_{gx} + x_{ci} \ddot{q}_{gy}) \\ + \sum_{i=1}^N m_i (-y_{ci} \ddot{q}_i + x_{ci} \ddot{q}_{N+i}) \\ + \ddot{q}_{0z} \sum_{i=1}^N m_i (y_{ci}^2 + x_{ci}^2) + \ddot{q}_{0z} \sum_{i=0}^N I_{zi} \\ + \ddot{\theta}_z \sum_{i=1}^N m_i (y_{ci}^2 + x_{ci}^2) + \ddot{\theta}_z \sum_{i=0}^N I_{zi} \\ + \sum_{i=1}^N m_i (y_{ci}^2 + x_{ci}^2 + I_{zi}) \ddot{q}_{2N+i} + M_{fz} = 0 \end{aligned} \tag{A1e}$$

Equations (A1 a) to (A1 e) can be expressed in a simplified form by the substitution of following terms:

$$\sum_{i=0}^N m_i = a \tag{A2a}$$

$$\sum_{i=1}^N m_i h_i = b \tag{A2b}$$

$$\sum_{i=1}^N (-m_i y_{ci}) = d_y \tag{A2c}$$

$$\sum_{i=0}^N I_{yi} + \sum_{i=1}^N m_i h_i^2 = c_y \tag{A2d}$$

$$\sum_{i=1}^N (-m_i y_{ci}) h_i = e_y \tag{A2e}$$

$$\sum_{i=1}^N m_i x_{ci} = d_x \tag{A2f}$$

$$\sum_{i=1}^N m_i x_{ci} h_i = e_x \tag{A2g}$$

$$\sum_{i=0}^N I_{zi} + \sum_{i=1}^N m_i (y_{ci}^2 + x_{ci}^2) = f \tag{A2h}$$

$$\sum_{i=0}^N I_{xi} + \sum_{i=1}^N m_i h_i^2 = c_x \tag{A2i}$$

and can be expressed as:

$$\begin{aligned} a \ddot{q}_{0x} + \sum_{i=1}^N m_i \ddot{q}_i + 0 + 0 \\ + b \ddot{\theta}_y + d_y \ddot{\theta}_z + \sum_{i=1}^N (-m_i y_{ci} \ddot{q}_{2N+i}) + V_{fx} \end{aligned} \tag{A3a}$$

$$\begin{aligned} = - a \ddot{q}_{gx} - d_y \ddot{q}_{0z} \\ b \ddot{q}_{0x} + \sum_{i=1}^N m_i \ddot{q}_i h_i + c_y \ddot{\theta}_y \\ + e_y \ddot{\theta}_z + \sum_{i=1}^N (-m_i y_{ci} \ddot{q}_{2N+i}) h_i + M_{fy} \\ = - b \ddot{q}_{gx} - e_y \ddot{q}_{0z} \end{aligned} \tag{A3b}$$

$$\begin{aligned} a \ddot{q}_{0y} + \sum_{i=1}^N m_i \ddot{q}_{N+i} + b \ddot{\theta}_x + d_x \ddot{\theta}_z \\ + \sum_{i=1}^N m_i x_{ci} \ddot{q}_{2N+i} + V_{fy} = - a \ddot{q}_{gy} - d_x \ddot{q}_{0z} \end{aligned} \tag{A3c}$$

$$\begin{aligned} b \ddot{q}_{0y} + \sum_{i=1}^N m_i \ddot{q}_{N+i} h_i + c_x \ddot{\theta}_x + e_x \ddot{\theta}_z + \sum_{i=1}^N (m_i x_{ci} \ddot{q}_{2N+i}) h_i \\ + M_{fx} = - b \ddot{q}_{gy} - e_x \ddot{q}_{0z} \end{aligned} \tag{A3d}$$

$$\begin{aligned}
 & d_y \ddot{q}_{0x} + d_x \ddot{q}_{0y} + e_y \ddot{\theta}_y + e_x \ddot{\theta}_x \\
 & + \sum_{i=1}^N m_i (y_{ci}^2 + x_{ci}^2 + I_{zi}) \ddot{q}_{2N+i} \\
 & + \sum_{i=1}^N -m_i y_{ci} \ddot{q}_i + \sum_{i=1}^N m_i x_{ci} \ddot{q}_{N+i} + f \ddot{\theta}_z + \\
 & + M_{fz} = -d_y q_{gx} - d_x q_{gy} - f \ddot{q}_{\theta z}
 \end{aligned} \tag{A3e}$$

Equations (A3a) to (A3e) may now be written in the matrix form as:

$$[B]^T [M] \{\ddot{q}\} + [K'_0] \{\ddot{q}_0\} + \{P_f\} = -[K'_1] \{\ddot{q}_g\} \tag{12}$$

in which

$$[K'_0] = \begin{bmatrix} a & 0 & b & 0 & d_y \\ 0 & a & 0 & b & d_x \\ b & 0 & c_y & 0 & e_y \\ 0 & b & 0 & c_y & e_x \\ d_y & d_x & e_y & e_x & f \end{bmatrix}$$

where $[K'_0]$ is a matrix, which when multiplied by $\{\ddot{q}_g\}$ gives the inertia forces produced by all masses of the structure and $\{P_f\}$ is a vector of reactive forces from the soil and can be expressed as:

$$\begin{aligned}
 & \begin{bmatrix} \overline{V}_{fx} \\ \overline{V}_{fy} \\ \overline{M}_{fy} \\ \overline{M}_{fx} \\ \overline{M}_{fz} \end{bmatrix} \\
 & = \begin{bmatrix} K_0''(1,1) & 0 & 0 & 0 & 0 \\ 0 & K_0''(2,2) & 0 & 0 & 0 \\ 0 & 0 & K_0''(3,3) & 0 & 0 \\ 0 & 0 & 0 & K_0''(4,4) & 0 \\ 0 & 0 & 0 & 0 & K_0''(5,5) \end{bmatrix} \\
 & \begin{bmatrix} \overline{q}_{0x} \\ \overline{q}_{0y} \\ \theta_y \\ \theta_x \\ \theta_z \end{bmatrix}
 \end{aligned}$$

where the non-zero terms $K_0''(i,j)$ are impedance functions in complex form defined as:

$$\begin{aligned}
 K_0''(1,1) &= k_x; K_0''(2,2) = k_y; K_0''(3,3) = k_{ry}; K_0''(4,4) \\
 &= k_{rx}; K_0''(5,5) = k_{rz}
 \end{aligned}$$

The values of k_x, k_y, k_{rx}, k_{ry} , and k_{rz} have been obtained from curves given by Wang and Luco [31].

References

- [1] Kozák J T 2009 Tutorial on earthquake rotational effects: Historical examples. *Bull. Seismol. Soc. Am.* 99: 998–1010
- [2] Zerva A, Falamarz-Sheikhabadi M R and Poul M K 2018 Issues with the use of spatially variable seismic ground motions in engineering applications. *Geotech. Geol. Earthq. Eng.* 46: 225–252
- [3] Hao H 1997 Torsional response of building structures to spatial random ground excitations. *Eng. Struct.* 19: 105–112
- [4] Hao H 1998 Response of two-way eccentric building to nonuniform base excitations. *Eng. Struct.* 20: 677–684
- [5] Hao H and Duan X N 1995 Seismic response of asymmetric structures to multiple ground motions. *J. Struct. Eng.* 121: 1557–1564
- [6] Hao H and Duan X 1996 Multiple excitation effects on response of symmetric buildings. *Eng. Struct.* 18: 732–740
- [7] De La Llera J C and Chopra A K 1994 Accidental and natural torsion in earthquake response and design of buildings. *UCB/EERC-94/07*
- [8] De la Llera J C and Chopra A K 1994 Accidental torsion in buildings due to base rotational excitation. *Earthq. Eng. Struct. Dyn.* 23: 1003–1021
- [9] Hao H 1996 Characteristics of torsional ground motions. *Earthq. Eng. Struct. Dyn.* 25: 599–610
- [10] Rambabu K V and Allam M M 2007 Response of an open-plane frame to multiple support horizontal seismic excitations with soil-structure interaction. *J. Sound Vib.* 299: 388–396
- [11] Gupta I D and Trifunac M D 2008 A note on contribution of torsional excitation to earthquake response of simple symmetric buildings. *Earthq. Eng. Eng. Vib.* 7: 27–46
- [12] Gupta V K and Trifunac M D 1990 Response of multistoried buildings to ground translation and rocking during earthquakes. *Probabilistic Eng. Mech.* 5: 138–145
- [13] Gupta V K and Trifunac M D 1990 A note on contributions of ground torsion to seismic response of symmetric multi-storied buildings. *Earthq. Eng. Eng. Vib.* 10: 27–40
- [14] Basu D, Whittaker A S and Constantinou M C 2012 *Characterizing the rotational components of earthquake ground motion*
- [15] Loghman V, Tajammolian H and Khoshnoudian F 2017 Effects of rotational components of earthquakes on seismic responses of triple concave friction pendulum base-isolated structures. *JVC/Journal Vib. Control* 23: 1495–1517
- [16] Basu D, Whittaker A S and Constantinou M C 2013 Extracting rotational components of earthquake ground motion using data recorded at multiple stations. *Earthq. Eng. Struct. Dyn.* 42: 451–468
- [17] Guidotti R, Castellani A and Stupazzini M 2018 Near-field earthquake strong ground motion rotations and their relevance on tall buildings. *Bull. Seismol. Soc. Am.* 108: 1171–1184
- [18] Poudel B, Özşahin E and Pekcan G 2022 Effect of Torsional Ground Motions on Floor Acceleration Response in Flexible SMRF Buildings. *J. Earthq. Eng.* 26: 2168–2185
- [19] Anagnostopoulos S A, Kyrkos M T and Stathopoulos K G 2015 Earthquake induced torsion in buildings: Critical review and state of the art. *Earthq. Struct.* 8: 305–377

- [20] Bhat J A, Ramana G V, Nagpal A K and Kamatchi P 2022 Effect of torsional ground motion on the seismic response of multistorey buildings on different soil mediums. *J. Struct. Eng.* 48: 467–484
- [21] Castellani A and Boffi G 1986 Rotational components of the surface ground motion during an earthquake. *Earthq. Eng. Struct. Dyn.* 14: 751–767
- [22] Schreiber K U, Velikoseltsev A, Carr A J and Franco-Anaya R 2009 The application of fiber optic gyroscopes for the measurement of rotations in structural engineering. *Bull. Seismol. Soc. Am.* 99: 1207–1214
- [23] Lee V W and Trifunac M D 1985 Torsional accelerograms. *Int. J. Soil Dyn. Earthq. Eng.* 4: 132–139
- [24] Oliveira C S and Bolt B A 1989 Rotational components of surface strong ground motion. *Earthq. Eng. Struct. Dyn.* 18: 517–526
- [25] Laouami N and Labbe P 2002 Experimental analysis of seismic torsional ground motion recorded by the LSST-Lotung array. *Earthq. Eng. Struct. Dyn.* 31: 2141–2148
- [26] Ghayamghamian M R and Nouri G R 2007 On the characteristics of ground motion rotational components using Chiba dense array data. *Earthq. Eng. Struct. Dyn.* 36: 1407–1429
- [27] O'Rourke M J, Bloom M C and Dobry R 1982 Apparent propagation velocity of body waves. *Earthq. Eng. Struct. Dyn.* 10: 283–294
- [28] Datta T K and Mashaly E A 1986 Pipeline response to random ground motion by discrete model. *Earthq. Eng. Struct. Dyn.* 14: 559–572
- [29] Lin J S 1987 Ground motion input through equivalent stationary motion. *Dev. Geotech. Eng.* 44: 537–549
- [30] Trifunac M D 1982 Rotational components of strong motion for incident body waves. *Int. J. Soil Dyn. Earthq. Eng.* 1: 11–19
- [31] Wong H L and Luco J E 1978 Tables of impedance functions and input motions for rectangular foundations. *Rep. - Univ. South. California, Dep. Civ. Eng.*
- [32] Bhat J 2004 *Effect of Torsional Ground Motion on the Seismic Response of Multistorey Buildings on Compliant Foundations*. Doctoral Dissertation, IIT Delhi, New Delhi (Indian Institute of Technology Delhi)
- [33] Wong H L and Luco J E 1976 Dynamic response of rigid foundations of arbitrary shape. *Earthq. Eng. Struct. Dyn.* 4: 579–587
- [34] Gazetas G 1991 Formulas and charts for impedances of surface and embedded foundations. *J. Geotech. Eng.* 117: 1363–1381